Organometallics 1991, 10, 1161-1172 1161

Center for Molecular Electronics for support of this work. We also wish to thank Prof. Robert R. Birge and Prof. Teresa B. Freedman for their assistance with this work.

Supplementary Material Available: Tables of complete MNDO-calculated bond lengths, bond angles, interplane dihedral angles, energy terms (electronic and thermodynamic data), and internal charge distribution data for compounds belonging to classes I–V (17 pages). Ordering information is given on any current masthead page.

Small Heteroborane Cluster Systems. 2.[1] Preparation of Phosphaborane Systems from the Reaction of Small Borane Cages with Low-Coordinate Phosphorus Compounds: Reaction Chemistry of Phosphaalkenes with Pentaborane(9)

Robert W. Miller, Kelley J. Donaghy, and James T. Spencer*

Department of Chemistry and Center for Molecular Electronics, Center for Science and Technology, Syracuse University, Syracuse, New York 13244-4100

Received August 29, 1990

The reaction of $(Me_3Si)P{=}C(R)(OSiMe_3)$ (where R = *tert*-butyl (**1a**) or adamantyl (**1b**)) with 1 equiv of neutral pentaborane(9), B_5H_9, under mild conditions produces the synthetically versatile, small bridging phosphaboranes $[\mu\text{-}((R)(Me_3SiO)HCP(SiMe_3))B_5H_8]$ (**2a**,**b**) in excellent yields. Two possible mechanisms for the formation of **2a** and **2b** by this reaction are supported by both experimental and MNDO semiempirical theoretical data. These relatively thermal and air-stable compounds are also stable with respect to the elimination of $Me_3SiOSiMe_3$. They are quantitatively converted, however, to $[\mu\text{-}((R)(Me_3SiO)CHP(X))B_5H_8]$ (where X = H (**3a**,**b**) and X = D (**4a**,**b**)) by electrophilic substitution reactions with water, D_2O, or alcohol. Compound **2a** is readily bridge-deprotonated by the action of NaH to produce the corresponding anion, $[\mu\text{-}((\textit{tert}\text{-butyl})(Me_3SiO)CHP(SiMe_3))B_5H_7]^-$ (**5a**), while **2b** is unreactive under similar conditions. Compound **5a** was found to be unreactive toward metal cations in complex formation. Compound **3a** slowly loses H_2 on standing at room temperature to form the bridged P=C system, $[\mu\text{-}((\textit{tert}\text{-butyl})(Me_3SiO)C{=}P)B_5H_8]$ (**6a**). Compound **3a** is readily cage-deprotonated to form the corresponding anion, $[\mu\text{-}((\textit{tert}\text{-butyl})(Me_3SiO)CHP(H))B_5H_7]^-$ (**7a**), which, when reacted with metal halides, forms metallaphosphaborane complexes. Data from MNDO calculations for compounds **2a**, **3a**, **5a**, and **6a** show linear relationships between the calculated charge on the bridgehead boron atoms and both the phosphorus–apical boron bond distance and the bridgehead basal boron bond centroid–phosphorus–carbon bond angle. These trends have been rationalized by using semiempirical molecular orbital considerations. Characterization of the new compounds was by ^1H, ^{11}B, ^{13}C, and ^{31}P NMR, infrared, mass spectral, and elemental analyses.

Introduction

An understanding of the important chemical relationships between bridged and inserted structures in substituted molecular clusters requires a detailed knowledge of the electronic structures and chemical features affecting these types of clusters. One class of polyhedral compounds in which these contributing factors can be carefully examined are the small heteroborane systems (with fewer than nine vertex atoms), specifically the phosphaboranes, since both theoretical and synthetic tools are either available or can be developed for their study. While several large phosphaborane systems have been previously reported, relatively little work has been done with systems with fewer than nine vertex boron atoms. It has been clearly demonstrated that the chemistry of large borane systems is significantly different from that of the smaller cages. The only small phosphaborane systems that have thus far been reported are several μ-phosphinopentaboranes by Burg,[2,3a,4] Gaines,[5] and Spencer,[3b] the *closo*-$P_2B_4Cl_4$ system,[6a] a P_2B_3 cage,[6b] two $C_{2n}B_4P_4$ (where n = 1 or 2) cages,[6c] and an inserted phosphahexaborane structure reported by Gaines.[5] Several terminally substituted phosphine–pentaborane species have also been reported.[6d] In addition, little is known about the reaction chemistry of these heteroborane systems.

The application of compounds containing both group III and V elements within a single species to the formation of thin-film materials by chemical vapor deposition (CVD) is an area of intense current interest.[7] Boron phosphide is particularly important as a III–V semiconductor in thermoelectric devices due to its wide band gap, high thermal conductivity, and high chemical stability.[8] The new compounds reported in this paper are potentially useful as CVD source materials for the formation of boron phosphide thin films.

In this paper, we report the rational high-yield synthesis and reaction chemistry of a family of synthetically versatile small phosphaboranes from the reaction of low-valent phosphorus compounds with pentaborane(9). These systems exhibit a wide diversity of substitution and elimi-

---

(1) Part 1: Glass, J. A., Jr.; Whelan, T. A.; Spencer, J. T. *Organometallics*, preceding paper in this issue.

(2) Burg, A. B. *Inorg. Chem.* **1973**, *12*, 3017.

(3) (a) Burg, A. B.; Heinen, H. *Inorg. Chem.* **1968**, *7*, 1021. (b) Miller, R. W.; Donaghy, K. J.; Spencer, J. T. *Phosphorus, Sulfur Silicon Relat. Elem.* **1991**, *57*, 287.

(4) Mishra, I. B.; Burg, A. B. *Inorg. Chem.* **1972**, *11*, 664.

(5) Coons, D. E.; Gaines, D. F. *Inorg. Chem.* **1987**, *26*, 1985.

(6) (a) Haubold, W.; Keller, W.; Sawitzki, G. *Angew. Chem., Int. Ed. Engl.* **1988**, *27*, 925. (b) Wood, G. L.; Duesler, E. N.; Narula, C. K.; Paine, R. T.; Noth, H. *J. Chem. Soc., Chem. Commun.* **1987**, *496*. (c) Driess, M.; Pritzkow, H.; Siebert, W. *Angew. Chem., Int. Ed. Engl.* **1988**, *27*, 399. (d) Kameda, M.; Kodama, G. *Inorg. Chem.* **1987**, *26*, 2011.

(7) Dowben, P. A.; Spencer J. T.; Stauf, G. T. *Mater. Sci. Eng. B* **1989**, *B2*, 297.

(8) Kumashiro, Y. *Rigaku J.* **1990**, *7*, 21.

0276-7333/91/2310-1161$02.50/0

nation reactions, including the elimination of hydrogen to form an unprecedented P=C bridged system. The proposed mechanism for the formation of these small phosphaboranes provides insights into the relationship between bridged and inserted structures. In this paper we have used semiempirical MNDO calculations in supporting mechanistic considerations and in gaining a deeper understanding into important structural relationships within these small heteroborane systems.

Experimental Section

Physical Measurements. Boron (^{11}B) NMR spectra were recorded on either a Bruker WM-360 or a Cryomagnetics spectrometer operating at 115.52 or 80.26 MHz, respectively. Spectra were recorded in either 5-mm or 10-mm (o.d.) tubes in both the coupled and decoupled modes and were externally referenced to BBr_3 at +40.0 ppm (positive chemical shifts indicate downfield resonances). Carbon (^{13}C) NMR spectra were obtained on a General Electric QE-300 spectrometer operating at 75.48 MHz. The spectrometer was operated in the FT mode while locked on the deuterium resonance of the $CDCl_3$ solvent in 5-mm (o.d.) sample tubes. The reference was set relative to tetramethylsilane from the known chemical shifts of the solvent carbon atoms. Phosphorus (^{31}P) NMR spectra were obtained in either 5-mm or 10-mm (o.d.) tubes on either a Bruker WM-360 or a Cryomagnetics spectrometer operating at 145.81 or 101.27 MHz, respectively. Chemical shifts were referenced to an external standard of 85% phosphoric acid sealed in a 1-mm capillary tube and held coaxially in the sample tube by a Teflon vortex plug. Both proton broad-band decoupled and coupled spectra were routinely observed for each sample with a decoupling power of about 5 W. Proton (^1H) NMR spectra were obtained on a General Electric QE-300 spectrometer operating at 300.15 MHz. Spectra were recorded on samples dissolved in $CDCl_3$ in 5-mm (o.d.) tubes with chemical shifts referenced to internal tetramethylsilane, with a positive shift indicating a resonance at an applied field lower than that of the standard. Mass spectra were obtained on a Finnigan 4021 mass spectrometer using an ionization potential of between 11 and 70 eV. Chemical ionization spectra were obtained by using methane as the bulk reactant gas. FT-IR spectra in the range of 4000 to 400 cm^{-1} were measured on either a Mattson Galaxy 2020 spectrometer or an IBM IR/32 spectrometer and were referenced to the 1601.8-cm^{-1} band of polystyrene. All compounds were recorded sandwiched between NaCl plates. HPLC purifications were accomplished on a Waters DeltaPrep-3000 system equipped with both tunable UV–vis absorbance (monitored routinely at 275 nm) and differential refraction detectors. All separations were performed by using a 2.5 × 10 cm RCM 15-μm porasil column and eluting with reagent grade solvents degassed by continuous He sparging. Elemental analyses were performed by Schwarzkopf Microanalytical Laboratories, Woodside, NY. Yields for pentaborane(9) reactions are reported on the basis of the initial amount of pentaborane used and the final isolated amount of the product obtained.

Materials. All solvents were reagent grade or better and were distilled from the appropriate drying agents under a dry nitrogen atmosphere prior to use: THF (Na), pentane (Na), and diethyl ether (Na). All organic solvents, after drying, were first degassed with a dry nitrogen stream followed by repeated freeze–thaw cycles and finally stored in vacuo prior to use. Deuterated solvents were used as received and, after degassing, were stored over 4-Å molecular sieves prior to use. Pentaborane(9) was from our laboratory stock. Tris(trimethylsilyl)phosphine, $P(SiMe_3)_3$, was prepared by a modification of the procedure reported in the literature.[9] The modification consisted of using 10% less than the stoichiometric amount of hexamethylphosphoramide (HMPA) and distilling the product directly from the reaction precipitate. This resulted in a significantly decreased amount of HMPA contamination in the final product, which, in turn, provided greater purity and higher yields for the new compounds reported here. $(Me_3Si)P{=}C(^tBu)(OSiMe_3)$[10] and $(Me_3Si)P{=}C(adamantyl)(OSiMe_3)$[11] were prepared by literature methods. The following commericially available (Aldrich) anhydrous chemicals were used either as received or purified by the method indicated and, where possible, were stored over 4-Å molecular sieves prior to use: HMPA, phosphorus trichloride, diglyme, chlorotrimethylsilane, magnesium metal, bromine, sodium hydroxide (dried at 150 °C under vacuum), 1-adamantanecarbonyl chloride, trimethylacyl chloride, methanol, hexafluoroboric acid, sodium hydride (the 80% suspension in mineral oil was washed several times with dry pentane and the washes decanted to remove the mineral oil), 2,6-lutidine (distilled). Analytical thin-layer chromatography was conducted on 2.5 × 7.5 cm silica gel strips (1B-F, Baker), and conventional column chromatography was conducted by using 2.5 × 30 cm columns packed with 230-400 mesh (ASTM) silica gel (EM Science).

Theoretical Calculations. The MNDO semiempirical calculations were performed by using either MOPAC 4.0 or MOPAC 5.0.[12] Parametrization for the atoms were those reported in the literature.[13] Our initial parameters and standard procedures for the determination of the MNDO-optimized structures for phosphapentaboranes have been reported previously and were followed in the work reported here.[1] No difficulties were encountered in the calculations.

$B_5H_8P(SiMe_3)(CH(OSiMe_3)(^tBu))$ (2a). In a typical reaction, 4.66 g of phosphaalkene **1a** (17.8 mmol) was placed in a 500-mL round-bottom reaction flask, which was connected via a Teflon vacuum stopcock to a high-vacuum manifold system (1 × 10^{-5} Torr). The oily material was degassed under vacuum for 30 min with continuous stirring. Into the reaction flask was condensed 1.12 g of pentaborane(9) (17.8 mmol) at −196 °C, and the reaction mixture was slowly warmed to 0 °C. The reaction was then allowed to warm slowly to room temperature over 5 h and stirred at this temperature for an additional 2 days. After this time, ^{11}B NMR analysis of the reaction mixture indicated the presence of only unreacted B_5H_9 and the new product **2a**. The unreacted B_5H_9 was readily removed under vacuum by trap-to-trap distillation at −196 °C. The slightly air-sensitive and moderately moisture-sensitive light orange-yellow oil thus obtained was found to be soluble in a variety of both polar and nonpolar organic solvents. The final yield of pure **2a** (4.74 g, 14.6 mmol) was 82%. Spectroscopic characterization for **2a** is given in Tables I and II. Anal. Calcd for $C_{11}H_{36}B_5OPSi_2$: C, 40.06; H, 11.14; P, 9.51; Si, 17.25. Found: C, 39.15; H, 10.36; P, 9.51; Si, 15.88. Electron impact mass spectroscopy of **2a** [parent ion relative intensities given with the largest peak in the envelope normalized to 100.0%; calculated values based on natural abundances and normalized to the most intense peak in the envelope; values in *m/e*]: 329 (calcd, 1.2; found 1.1; P^+ envelope), 328 (calcd, 7.9; found, 5.6; P^+ envelope), 327 (calcd, 25.1; found, 20.9; P^+ envelope), 326 (calcd, 95.8; found, 94.5; $^{12}C_{11}{}^1H_{36}{}^{11}B_5{}^{16}O^{31}P^{28}Si_2$; P^+ envelope), 325 (calcd, 100.0; found, 100.0; P^+ envelope), 324 (calcd, 47.4; found, 45.5; P^+ envelope), 323 (calcd, 11.0; found, 8.9; P^+ envelope), 322 (calcd, 1.2; found, 1.0; P^+ envelope), 168 (calcd, 2.8; found, 4.5; $P^+ - R$ envelope), 167 (calcd, 21.0; found, 38.7; $^{12}C_3{}^1H_{17}{}^{11}B_5{}^{31}P^{28}Si_1$; $P^+ -$ R envelope), 166 (calcd, 44.9; found, 44.9; $P^+ - R$ envelope), 165 (calcd, 38.7; found, 22.0; $P^+ - R$ envelope), 164 (calcd, 16.9; found, 5.3; $P^+ - R$ envelope), 163 (calcd, 4.1; found, 0.5; $P^+ - R$ envelope), 161 (calcd, 4.4; found, 4.1; $C(OSiMe_3)(^tBu)H^+$), 160 (calcd, 14.3; found, 13.5; $C(OSiMe_3)(^tBu)H^+$), 159 (calcd, 100.0; found, 100.0; $C(OSiMe_3)(^tBu)H^+$, $^{12}C_8{}^1H_{19}{}^{16}O^{28}Si$).

$B_5H_8P(SiMe_3)(CH(OSiMe_3)(adamantyl))$ (2b). This compound was prepared in a manner directly analogous to that used for **2a**, except that 17.0 g (50 mmol) phosphaalkene **1b** was reacted with 3.15 g (50 mmol) of pentaborane(9). The final yield of **2b** (19.1 g, 47.2 mmol) was 94%. The product was recrystallized from

---

[9] Schumann, H.; Rosch, L. *J. Organomet. Chem.* **1973**, *55*, 257.

[10] Becker, G. *Z. Anorg. Allg. Chem.* **1977**, *430*, 66.

[11] Allspach, T.; Regitz, M.; Becker, G.; Becker, W. *Synthesis* **1986**, 31.

[12] Stewart, J. J. P.; Seiler, F. J. *Quantum Chem. Program Exch.* Program No. 455.

[13] Parametrizations used for the MNDO calculations were: (a) Dewar, M. J. S.; McKee, M. L. *J. Am. Chem. Soc.* **1977**, *99*, 5231 (boron). (b) Dewar, M. J. S.; Theil, W. *J. Am. Chem. Soc.* **1977**, *99*, 4899 (hydrogen, carbon, and oxygen). (c) Dewar, M. J. S.; McKee, M. L.; Rzepa, H. S. *J. Am. Chem. Soc.* **1978**, *100*, 3607 (phosphorus). (d) Dewar, M. J. S.; Freidheim, J.; Grady, G.; Healy, E. F.; Stewart, J. J. P. *Organometallics* **1986**, *5*, 375 (silicon).

dry toluene at -10 °C to obtain a colorless, microcrystalline material. Spectroscopic characterization for this compound is given in Tables I and II. Electron impact mass spectroscopy for **2b** [parent ion relative intensities are given with the largest peak in the envelope normalized to 100.0%; calculated values based on natural abundances and normalized to the most intense peak in the envelope; values in *m*/*e*]: 407 (calcd, 1.7; found, 1.2; P^+ envelope), 406 (calcd, 9.5; found, 9.3; P^+ envelope), 405 (calcd, 30.8; found, 26.7; P^+ envelope), 404 (calcd, 99.3; found, 89.6; $^{12}C_{17}{}^{1}H_{42}{}^{11}B_5{}^{16}O^{31}P^{28}Si_2$; P^+ envelope), 403 (calcd, 100.0; found, 100.0; P^+ envelope), 402 (calcd, 46.4; found, 46.4; P^+ envelope), 401 (calcd, 11.6; found, 12.4; P^+ envelope), 400 (calcd, 1.4; found, 4.3; P^+ envelope), 239 (calcd, 5.5; found, 3.8; $C(OSiMe_3)(Ad)H^+$), 238 (calcd, 21.1; found, 18.3; $C(OSiMe_3)$(adamantyl)H^+), 237 (calcd, 100.0; found, 100.0; $C(OSiMe_3)$(adamantyl)H^+, $^{12}C_{14}{}^{1}H_{25}{}^{16}O^{28}Si$), 168 (calcd, 1.1; found, 0.4; $P^+ - R$ envelope), 167 (calcd, 9.3; found, 2.8; $^{12}C_3{}^{1}H_{17}{}^{11}B_5{}^{31}P^{28}Si$; $P^+ - R$ envelope), 166 (calcd, 10.8; found, 10.8; $P^+ - R$ envelope), 165 (calcd, 5.3; found, 8.7; $P^+ - R$ envelope), 164 (calcd, 1.3; found; 4.7; $P^+ - R$ envelope), 163 (calcd, 0.1; found, 1.0; $P^+ - R$ envelope).

$B_5H_8P(H)(CH(OSiMe_3)(^tBu))$ (3a). Under an inert nitrogen atmosphere, 0.22 g (0.68 mmol) of **2a** was dissolved in 5 mL of dry THF. To this solution was added by syringe 12 μL (0.7 mmol) of water. Vigorous bubbling began immediately and continued for several minutes. The solvent was removed in vacuo to leave an off-white solid. The product was further purified employing either standard column chromatographic or HPLC chromatographic procedures (HPLC parameters 2.5 × 10 cm 15-μm porasil column eluted with 100% methylene chloride with a flow rate of 7 mL/min.; **3a** eluted from the column in 5.6 min). The final product was obtained as a white, relatively air-stable oil in near quantitative conversion from **2a** (0.16 g, 93.4% yield). The addition of excess water significantly decreases the yield of **3a** obtained. An alternative method for the preparation of **3a** was to dissolve compound **2a** in 5 mL of methylene chloride and pass this solution rapidly down a 2.5 × 2.5 cm silica gel column eluted with 50 mL of methylene chloride. The product was collected as a single band, and the solvent was removed in vacuo to yield pure **3a**. Spectroscopic characterization for **3a** is given in Tables I and II. Electron impact mass spectroscopy for **3a** [parent ion relative intensities are given with the largest peak in the envelope normalized to 100.0%; calculated values based on natural abundances and normalized to the most intense peak in the envelope; values in *m*/*e*]: 256 (calcd, 3.6; found, 2.5; P^+ envelope), 255 (calcd, 14.7; found, 12.6; P^+ envelope), 254 (calcd, 89.7; found, 86.2; $^{12}C_8{}^{1}H_{28}{}^{11}B_5{}^{16}O^{31}P^{28}Si$; P^+ envelope), 253 (calcd, 100.0; found, 100.0; P^+ envelope), 252 (calcd, 48.1; found, 47.4; P^+ envelope), 251 (calcd, 11.8; found, 10.7; P^+ envelope), 250 (calcd, 1.5; found, 1.0; P^+ envelope), 161 (calcd, 4.4; found, 3.9; $C(OSiMe_3)(^tBu)H^+$), 160 (calcd, 14.3; found, 12.9; $C(OSiMe_3)(^tBu)H^+$), 159 (calcd, 100.0; found, 100.0; $C(OSiMe_3)(^tBu)H^+$, $^{12}C_8{}^{1}H_{19}{}^{16}O^{28}Si$).

Samples of **3a** were slowly converted to a new compound on standing at room temperature. This compound, **6a**, was purified by using HPLC procedures (HPLC parameters 2.5 × 10 cm 15-μm porasil column eluted with 100% methylene chloride with a flow rate of 7 mL/min; **6a** eluted from the column in 5.9 min). The product was obtained in 52% yield (based on ^{11}B NMR analysis) as a colorless, relatively air-stable oily material. Spectroscopic characterization for **6a** is given in Tables I and II. Electron impact mass spectroscopy for **6a** [calculated values based on natural abundances and normalized to the most intense peak in the envelope; value in *m*/*e*]: 254 (calcd, 0.04; found, 0.03; P^+ envelope), 253 (calcd, 0.2; found, 0.6; P^+ envelope), 252 (calcd, 1.1; found, 1.1; $^{12}C_8{}^{1}H_{26}{}^{11}B_5{}^{16}O^{31}P^{28}Si$; P^+ envelope), 251 (calcd, 1.2; found, 0.8; P^+ envelope), 250 (calcd, 0.6; found, 1.0; P^+ envelope), 249 (calcd, 0.2; found, 0.8; P^+ envelope).

A similar reaction for **3b** was also observed to occur to form compound **6b**.

$B_5H_8P(H)(CH(OSiMe_3)$(adamantyl)) (3b). Compound **3b** was prepared in a manner directly analogous to that used for **3a**. In a typical experiment 5.23 g (12.9 mmol) of **2b** was dissolved in 5 mL of methylene chloride and the solution was quickly passed down a 2.5 × 15 cm silica gel column, which was eluted with pure methylene chloride. Compound **3b** was collected as a white solid in quantitative conversion from **2b**. HPLC chromatographic procedures were used to purify the product (HPLC parameters 2.5 × 10 cm 15-μm porasil column eluted with 100% methylene chloride with a flow rate of 7 mL/min; **3a** eluted from the column in 5.7 min). Spectroscopic characterization for **3b** is given in Tables I and II. Electron impact mass spectroscopy for **3b** [calculated values based on natural abundances and normalized to the most intense peak in the envelope; values in *m*/*e*]: 334 (calcd, 0.6; found, 6.1; P^+ envelope), 333 (calcd, 3.1; found, 8.9; P^+ envelope), 332 (calcd, 14.2; found, 10.5; $^{12}C_{14}{}^{1}H_{34}{}^{11}B_5{}^{16}O^{31}P^{28}Si$; P^+ envelope), 331 (calcd, 15.3; found, 15.3; P^+ envelope), 330 (calcd, 7.2; found, 1.7; P^+ envelope), 329 (calcd, 1.7; found, 0.7; P^+ envelope), 328 (calcd, 0.2; found, 0.4; P^+ envelope), 239 (calcd, 5.5; found, 5.1; $C(OSiMe_3)$(adamantyl)H^+), 238 (calcd, 21.1; found, 20.2; $C(OSiMe_3)$(adamantyl)H^+), 237 (calcd, 100.0; found, 100.0; $C(OSiMe_3)$(adamantyl)H^+, $^{12}C_{14}{}^{1}H_{25}{}^{16}O^{28}Si$), 95 (calcd, 80.1; found, 37.2; $^{1}H_9{}^{11}B_5{}^{31}P$; B_5H_8PH envelope), 94 (calcd, 100; found, 74.7; B_5H_8PH envelope), 93 (calcd, 50.0; found, 100; B_5H_8PH envelope), 92 (calcd, 12.5; found, 75.9; B_5H_8PH envelope), 91 (calcd, 1.6; found, 11.4; B_5H_8PH envelope).

$B_5H_8P(D)(CH(OSiMe_3)(^tBu))$ (4a) and $B_5H_8P(D)(CH(OSiMe_3)$(adamantyl)) (4b). In a 5-mm (o.d.) NMR tube and under an inert nitrogen atmosphere was placed 0.02 g of either compound **2a** or **2b**. The compound was dissolved in 0.5 mL of dry, degassed chloroform-d_1 added by means of a syringe through the tube's septum. To this solution was then added by syringe 1 drop of D_2O. Vigorous bubbling was observed upon the D_2O addition, which subsided within a few minutes. Spectroscopic measurements were obtained on this sample and are tabulated in Tables I and II. Electron impact mass spectroscopy for **4a** [calculated values based on natural abundances and normalized to the most intense peak in the envelope; values in *m*/*e*]: 255 (calcd, 20.3; found, 15.0; $^{12}C_8{}^{1}H_{27}{}^{2}H_1{}^{11}B_5{}^{16}O^{31}P^{28}Si$; P^+ envelope), 254 (calcd, 26.6; found, 26.6; P^+ envelope), 253 (calcd, 10.8; found, 17.6; P^+ envelope), 161 (calcd, 3.9; found, 4.5; $C(OSiMe_3)(^tBu)H^+$), 160 (calcd, 14.3; found, 13.4; $C(OSiMe_3)(^tBu)H^+$), 159 (calcd, 100.0; found, 100.0; $C(OSiMe_3)(^tBu)H^+$, $^{12}C_8{}^{1}H_{19}{}^{16}O^{28}Si$), 96 (calcd, 1.4; found, 1.8; $^{1}H_8{}^{2}H_1{}^{11}B_5{}^{31}P$; B_5H_8PD envelope), 95 (calcd, 1.8; found, 0.5; B_5H_8PD envelope), 94 (calcd, 0.9; found, 1.1; B_5H_8PD envelope). Negative ion mass spectroscopy for **4b** [parent ion relative intensities are given with the largest peak in the envelope normalized to 100.0%; values in *m*/*e*]: 334 (calcd, 20.6; found, 32.2; P^+ envelope), 333 (calcd, 93.5; found, 100; P^+ envelope), 332 (calcd, 100; found, 92.2; $^{12}C_{14}{}^{1}H_{33}{}^{2}H_1{}^{11}B_5{}^{16}O^{31}P^{28}Si$; P^+ envelope), 331 (calcd, 47.4; found, 57.7; P^+ envelope), 330 (calcd, 11.5; found, 37.3; P^+ envelope), 329 (calcd, 1.4; found, 0.5; P^+ envelope), 137 (calcd, 0.6; found, 4.5; adamantyl ion), 136 (calcd 11.3; found, 18.6; adamantyl ion), 135 (calcd, 100.0; found, 100.0; adamantyl ion $^{12}C_{10}{}^{1}H_{15}$).

The addition of water to either **4a** or **4b** did not produce **3a** or **3b**, indicating the relative nonlability of the H–P linkage.

Reaction of $B_5H_8P(SiMe_3)(CH(OSiMe_3)(^tBu))$ (2a) with Methanol. In a manner analogous to that used for the preparation of **4a** and **4b**, 0.02 g of **2a** was placed in a 5-mm (o.d.) NMR tube in 0.5 mL of chloroform-d_1 and reacted with 1 drop of dry, degassed methanol. After the vigorous bubbling had ceased, spectroscopic analysis of the solution indicated the formation of compound **3a**.

$[B_5H_7P(SiMe_3)(CH(OSiMe_3)(^tBu))](1-)$ (5a). Into a 15-mL side-arm tube, equipped with a high-vacuum stopcock and attached to a 200-mL round-bottom flask, was placed 0.27 g (0.79 mmol) of dried and degassed compound **2a**. In the 200-mL round-bottom flask was placed 0.024 g (1.25 equiv, 0.99 mmol) of dry, pure NaH, which had been carefully washed with excess pentane and dried in vacuo. The reaction system was evacuated to 10^{-3} Torr, and 20 mL of THF was condensed into the reaction flask. Approximately 5 mL of THF was then condensed into the side-arm tube to dissolve **2a**. The solution of **2a** was added in one portion to the NaH at room temperature. Gas evolution was observed upon addition of the solution to the NaH. After approximately 20 min, the gas evolution had subsided and the solution was filtered through a glass frit under inert conditions to yield a clear, light yellow solution. The solvent was removed in vacuo from the filtrate to leave an oily residue. Spectroscopic characterization for **5a** is given in Tables I and II. The anion was stored under vacuum at -78 °C until required.

It was found, through repeated attempts, that it was not possible to deprotonate compound **2b** under any reaction condition

Table I. NMR Data (ppm) for Bridging Phosphaborane Systems

compd	^{11}B data[a]	^{1}H data[b]	^{13}C{^{1}H} data[c,d]	^{31}P data[e]	ref
$\mathrm{P(SiMe_3)_3}$		0.29 (d, 9 H, $\mathrm{Si}(\mathrm{C}H_3)_3$, J_{PH} = 4.5 Hz)	3.93 (s, $\mathrm{Si}(C\mathrm{H}_3)_3$, J_{CP} = 11.2 Hz)	−251.0	this work[f]
1a (E isomer)		0.27 (d, 9 H, $\mathrm{PSi}(\mathrm{C}H_3)_3$, J_{PH} = 3.9 Hz), 0.36 (s, 9 H, $\mathrm{OSi}(\mathrm{C}H_3)_3$), 1.24 (d, 9 H, $\mathrm{C}(\mathrm{C}H_3)_3$, J_{PH} = 0.9 Hz)	0.9 (d, $\mathrm{PSi}(C\mathrm{H}_3)_3$, J_{PC} = 8.1 Hz), 2.0 (s, $\mathrm{PSi}(C\mathrm{H}_3)_3$), 30.7 (d, $\mathrm{C}(C\mathrm{H}_3)_3$, J_{PC} = 2.0 Hz), 45.2 (d, $C(\mathrm{CH}_3)_3$, J_{PC} = 12.2 Hz), 229.0 (d, P*C*, J_{PC} = 80.6 Hz)	124.0	^{13}C, ^{31}P, ref 30; ^{1}H, this work[g]
1a (Z isomer)		0.23 (s, 9 H, $\mathrm{OSi}(\mathrm{C}H_3)_3$), 0.32 (d, 9 H, $\mathrm{PSi}(\mathrm{C}H_3)_3$, J_{PH} = 3.9 Hz), 1.24 (d, 9 H, $\mathrm{C}(\mathrm{C}H_3)_3$, J_{PH} = 1.5 Hz)	0.92 (d, $\mathrm{PSi}(C\mathrm{H}_3)$, J_{PC} = 10.0 Hz), 2.33 (s, $\mathrm{OSi}(C\mathrm{H}_3)_3$), 30.15 (d, $\mathrm{C}(C\mathrm{H}_3)_3$, J_{PC} = 12.6 Hz), 45.15 (d, $C(\mathrm{CH}_3)_3$, J_{PC} = 23.9 Hz), 225.80 (d, P*C*, J_{PC} = 80.4 Hz)	121.2	this work[g]
1b (Z isomer)		0.27 (d, 9 H, $\mathrm{PSi}(\mathrm{C}H_3)_3$, J_{PH} = 3.9 Hz), 0.38 (s, 9 H, $\mathrm{OSi}(\mathrm{C}H_3)_3$), 1.60–2.10 (m, 15 H, $\mathrm{C}_{10}H_{15}$)	1.04 (d, $\mathrm{PSi}(C\mathrm{H}_3)_3$, J_{CP} = 9.9 Hz), 2.62 (s, $\mathrm{OSi}(C\mathrm{H}_3)_3$), 28.62 (d, $\mathrm{C}_{10}\mathrm{H}_{15}$, C_{B}, J_{CP} = 1.6 Hz), 36.53 (s, $\mathrm{C}_{10}\mathrm{H}_{15}$, C_{C}), 41.45 (d, $\mathrm{C}_{10}\mathrm{H}_{15}$, C_{A}, J_{CP} = 13.6 Hz), 47.15 (d, $\mathrm{C}_{10}\mathrm{H}_{15}$, C_{D}, J_{CP} = 21.4 Hz), 227.78 (d, P*C*, J_{PC} = 76.6 Hz)	120.5	this work[h]
2a	−2.2 (s, B(4,5)), −19.6 (s, B(2,3)), −48.6 (d, B(1), J_{BH} = 152 Hz)	−1.75 (s, 3 H, bridging H), −0.37 (q, 1 H, B(1)*H*, J_{BH} = 150.3 Hz), 0.17 (s, 9 H, $\mathrm{OSi}(\mathrm{C}H_3)_3$), 0.49 (d, 9 H, $\mathrm{PSi}(\mathrm{C}H_3)_3$, J_{PH} = 5.4 Hz), 0.92 (s, 9 H, $\mathrm{C}(\mathrm{C}H_3)_3$), 3.49 (d, 1 H, PC*H*, J_{PH} = 7.5 Hz)	0.11 (d, $\mathrm{PSi}(C\mathrm{H}_3)_3$, J_{CP} = 9.2 Hz), 0.93 (s, $\mathrm{OSi}(C\mathrm{H}_3)_3$), 26.99 (d, $\mathrm{C}(C\mathrm{H}_3)_3$, J_{CP} = 4.3 Hz), 37.31 (d, $C(\mathrm{CH}_3)_3$, J_{CP} = 3.6 Hz), 78.24 (d, P*C*, J_{CP} = 10.5 Hz)	−124.5 (s)	this work
2b	−2.7 (s, B(4,5)), −19.4 (s, B(2,3)), −48.2 (d, B(1), J_{BH} = 147 Hz)	−1.70 (s, 3 H, bridging H), −0.40 (q, 1 H, B(1)*H*, J_{BH} = 147.9 Hz), 0.16 (s, 9 H, $\mathrm{OSi}(\mathrm{C}H_3)_3$), 0.49 (d, 9 H, $\mathrm{PSi}(\mathrm{C}H_3)_3$), J_{PH} = 5.4 Hz), 1.57–2.35 (m, 15 H, $\mathrm{C}_{10}H_{15}$), 3.28 (d, 1 H, PC*H*, J_{PH} = 6.6 Hz)	0.20 (d, $\mathrm{PSi}(C\mathrm{H}_3)_3$, J_{CP} = 7.8 Hz), 0.92 (s, $\mathrm{OSi}(C\mathrm{H}_3)_3$), 28.30 (s, $\mathrm{C}_{10}\mathrm{H}_{15}$, C_{B}), 36.89 (s, $\mathrm{C}_{10}\mathrm{H}_{15}$, C_{C}), 39.18 (d, $\mathrm{C}_{10}\mathrm{H}_{15}$, C_{D}, J_{CP} = 4.1 Hz), 39.38 (d, $\mathrm{C}_{10}\mathrm{H}_{15}$, C_{A}, J_{CP} = 2.0 Hz), 79.20 (d, P*C*, J_{CP} = 8.8 Hz)	−127.9 (s)	this work
3a	−1.6 (d, B(4,5), J_{BH} = 156 Hz), −22.0 (t, B(2,3), J_{BP} = 82 Hz, J_{BH} = 80 Hz), −47.5 (d, B(1), J_{BH} = 152 Hz)	−1.80 (br s, 2 H, bridging H), −1.40 (br s, 1 H, bridging H), −0.04 (q, 1 H, B(1)*H*, J_{BH} = 152.3 Hz), 0.17 (s, 9 H, $\mathrm{OSi}(\mathrm{C}H_3)_3$), 1.00 (s, 9 H, $\mathrm{C}(\mathrm{C}H_3)_3$), 3.33 (dd, 1 H, PC*H*, J_{PH} = 7.2 Hz, J_{HH} = 3.0 Hz), 5.27 (d, 1 H, P*H*, J_{PH} = 410 Hz)	0.76 (s, $\mathrm{OSi}(C\mathrm{H}_3)_3$), 26.57 (d, $\mathrm{C}(C\mathrm{H}_3)_3$, J_{CP} = 4.8 Hz), 37.24 (s, $C(\mathrm{CH}_3)_3$), 79.64 (s, P*C*)	−97.5 (d, J_{PH} = 410 Hz)	this work
3b	−1.1 (d, B(4,5), J_{BH} = 153 Hz), −21.6 (t, B(2,3), J_{BP} = 77 Hz, J_{BH} = 99 Hz), −46.5 (d, B(1), J_{BH} = 155 Hz)	−1.70 (br s, 2 H, bridging H), −1.40 (br s, 1 H, bridging H), −0.12 (q, 1 H, B(1)*H*, J_{BH} = 150.4 Hz), 0.17 (s, 9 H, $\mathrm{OSi}(\mathrm{C}H_3)_3$), 1.50–2.10 (m, 15 H, $\mathrm{C}_{10}H_{15}$), 3.91 (dd, 1 H, PC*H*, J_{HH} = 2.7 Hz, J_{PH} = 6.3 Hz), 5.32 (d, 1 H, P*H*, J_{PH} = 406 Hz)	0.80 (s, $\mathrm{OSi}(C\mathrm{H}_3)_3$), 28.16 (s, $\mathrm{C}_{10}\mathrm{H}_{15}$, C_{B}), 36.81 (s, $\mathrm{C}_{10}\mathrm{H}_{15}$, C_{C}), 38.79 (d, $\mathrm{C}_{10}\mathrm{H}_{15}$, C_{D}, J_{CP} = 6.1 Hz), 39.22 (s, $\mathrm{C}_{10}\mathrm{H}_{15}$, C_{A}), 79.80 (d, P*C*, J_{CP} = 5.2 Hz)	−101.0 (d, J_{PH} = 406 Hz)	this work
4a	−1.8 (d, B(4,5), J_{BH} = 158 Hz), −22.4 (t, B(2,3), J_{BP} = 81 Hz, J_{BH} = 104 Hz), −47.5 (d, B(1), J_{BH} = 155 Hz)	−1.80 (br s, 2 H, bridging H), −1.45 (br s, 1 H, bridging H), −0.10 (q, 1 H, B(1)*H*, J_{BH} = 150.0 Hz), 0.16 (s, 9 H, $\mathrm{OSi}(\mathrm{C}H_3)_3$), 0.99 (s, 9 H, $\mathrm{C}(\mathrm{C}H_3)_3$), 1.89 (q, 2 H, B(4,5)*H*, J_{BH} = 146.3 Hz), 3.33 (d, 1 H, PC*H*, J_{PH} = 6.9 Hz)	0.76 (s, $\mathrm{OSi}(C\mathrm{H}_3)_3$), 26.55 (d, $\mathrm{C}(C\mathrm{H}_3)_3$, J_{CP} = 4.8 Hz), 37.26 (s, $C(\mathrm{CH}_3)_3$), 79.58 (s, P*C*)	−102.4 (br s)	this work
4b	−1.0 (d, B(4,5), J_{BH} = 147 Hz), −21.4 (t, B(2,3), J_{BP} = 73 Hz, J_{BH} = 100 Hz), −46.5 (d, B(1), J_{BH} = 157 Hz)	−1.85 (br s, 2 H, bridging H), −1.50 (br s, 1 H, bridging H), −0.45 (q, 1 H, B(1)*H*, J_{BH} = 160.0 Hz), 0.15 (s, 9 H, $\mathrm{OSi}(\mathrm{C}H_3)_3$), 1.40–2.10 (m, 15 H, $\mathrm{C}_{10}H_{15}$), 3.17 (d, 1 H, PC*H*, J_{PH} = 6.3 Hz)	0.80 (s, $\mathrm{OSi}(C\mathrm{H}_3)_3$), 28.21 (s, $\mathrm{C}_{10}\mathrm{H}_{15}$, C_{B}), 36.86 (s, $\mathrm{C}_{10}\mathrm{H}_{15}$, C_{C}), 38.81 (d, $\mathrm{C}_{10}\mathrm{H}_{15}$, C_{D}, J_{CP} = 4.7 Hz), 39.20 (s, $\mathrm{C}_{10}\mathrm{H}_{15}$, C_{A}), 79.69 (d, P*C*, J_{CP} = 3.8 Hz)	−106.3 (br s)	this work
5a	−1.9 (s, B(4,5)), −18.7 (s, B(2,3)), −48.4 (d, B(1), J_{BH} = 157 Hz)	−1.72 (s, 2 H, bridging H), −0.68 (q, 1 H, B(1)*H*, J_{BH} = 150.0 Hz), 0.17 (s, 9 H, $\mathrm{OSi}(\mathrm{C}H_3)_3$), 0.49 (d, 9 H, $\mathrm{PSi}(\mathrm{C}H_3)_3$), J_{PH} = 5.4 Hz), 0.92 (s, 9 H, $\mathrm{C}(\mathrm{C}H_3)_3$), 3.49 (d, 1 H, PC*H*, J_{PH} = 7.2 Hz)	0.10 (d, $\mathrm{PSi}(C\mathrm{H}_3)_3$, J_{CP} = 8.1 Hz), 0.91 (s, $\mathrm{OSi}(C\mathrm{H}_3)_3$), 26.93 (d, $\mathrm{C}(C\mathrm{H}_3)_3$, J_{CP} = 4.3 Hz), 37.26 (d, $C(\mathrm{CH}_3)_3$, J_{CP} = 3.6 Hz), 78.28 (d, P*C*, J_{CP} = 9.7 Hz)	−124.3 (s)	this work
6a	−1.0 (d, B(4,5), J_{BH} = 143 Hz), −9.9 (t, B(2/3), J_{BP} = 111 Hz, J_{BH} = 152 Hz), −12.3 (t, B(2/3), J_{BP} = 97 Hz, J_{BH} = 147 Hz), −47.5 (d, B(1), J_{BH} = 159 Hz)	−1.70 (br s, 3 H, bridging H), −0.34 (q, 1 H, B(1)*H*, J_{BH} = 153.7 Hz), 0.07 (s, 9 H, $\mathrm{OSi}(\mathrm{C}H_3)_3$), 1.28 (s, 9 H, $\mathrm{C}(\mathrm{C}H_3)_3$)	1.02 (s, $\mathrm{OSi}(C\mathrm{H}_3)_3$), 29.70 (s, $\mathrm{C}(C\mathrm{H}_3)_3$), 31.92 (s, $C(\mathrm{CH}_3)_3$), 148.49 (br s, P=*C*)	26.1	this work

Table I (Continued)

compd	^{11}B data[a]	^{1}H data[b]	^{13}C{^{1}H} data[c,d]	^{31}P data[e]	ref
7a	0.3 (d, B(4,5), J_{BH} = 146 Hz), −20.7 (br s, B(2,3), −45.3 (d, B(1), J_{BH} = 150 Hz)	−1.86 (br s, 2 H, bridging H), −0.15 (q, 1 H, B(1)*H*, J_{BH} = 152.7 Hz), 0.16 (s, 9 H, OSi(C*H*$_3$)$_3$), 0.99 (s, 9 H, C(C*H*$_3$)$_3$), 1.80 (q, 2 H, B(4,5)*H*, J_{BH} = 150.0 Hz), 3.33 (dd, 1 H, PC*H*, J_{PH} = 5.6 Hz, J_{HH} = 2.5 Hz), 5.28 (d, 1 H, P*H*, J_{PH} = 421 Hz)	0.75 (s, OSi(*C*H$_3$)$_3$), 26.57 (d, C(*C*H$_3$)$_3$, J_{CP} = 4.8 Hz), 37.26 (s, *C*(CH$_3$)$_3$), 79.65 (s, P*C*)	−97.4 (d, J_{PH} = 421 Hz)	this work

[a] In CDCl$_3$ relative to BBr$_3$ (40.0 ppm). [b] In CDCl$_3$ relative to TMS. [c] In CDCl$_3$ relative to TMS. [d] adamantyl numbering scheme:

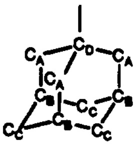

[e] In CDCl$_3$ relative to 85% H$_3$PO$_4$. [f] ^{1}H and ^{31}P data for this compound were reported in ref 31. The data shown here are our data, which are comparable with those reported earlier. [g] ^{13}C, ^{1}H, and ^{31}P data for this compound were originally reported in ref 10. The data shown here are our data, which are comparable with those reported earlier. [h] ^{13}C, ^{1}H, and ^{31}P data for this compound were originally reported in ref 11. The data shown here are our data, which are comparable with those reported earlier.

investigated and that only unreacted starting materials were recovered from all attempts.

Reaction of (Me$_3$Si)P═C(OSiMe$_3$)(^{t}Bu) (1a) with B$_5$H$_8$$^-$. In a typical experiment, a solution of Na$^+$[B$_5$H$_8$]$^-$ was prepared in vacuo from the reaction of 0.063 g (1.0 mmol) of B$_5$H$_9$ with 0.030 g (1.25 mmol) of NaH in 20 mL of THF at −20 °C by using standard techniques.[14,15] ^{11}B NMR characterization of the solution showed the presence of Na$^+$[B$_5$H$_8$]$^-$. The cold Na$^+$[B$_5$H$_8$]$^-$ solution was filtered through a glass frit into a 500-mL flask containing 0.27 g (1.0 mmol) of compound 1a at −196 °C. The reaction mixture was allowed to warm slowly and to stir at −20 °C for 3 h. An aliquot was removed from the reaction mixture and was analyzed by NMR spectroscopy. It consisted entirely of the Na$^+$[B$_5$H$_8$]$^-$ decomposition product B$_9$H$_{14}$$^-$.[16]

[B$_5$H$_7$P(H)(CH(OSiMe$_3$)(^{t}Bu))](1−) (7a) and [B$_5$H$_7$P(H)(CH(OSiMe$_3$)(adamantyl))](1−) (7b). In the side-arm tube of an apparatus similar to that described for the preparation of **5a** was placed 1.6 g (3.0 mmol) of **3a**. The connected round-bottom flask was charged with 0.11 g (4.5 mmol, 1.5 equiv) of hexane-washed NaH. The reaction apparatus was evacuated to 10^{-3} Torr, and 10 mL of dry, degassed THF was condensed onto the NaH and 10 mL into the side-arm tube. The THF solutions were warmed to room temeratuure, and the solution of **3a** was added to the NaH. Vigorous gas evolution was observed to begin immediately. After 1 h at room temperature the bubbling had ceased and the solvent was removed in vacuo to leave an oily residue. Spectroscopic characterization for **7a** is given in Tables I and II. The anion was stored under vacuum at −78 °C until required.

A similar reaction for **3b** was observed to occur to form compound **7b**.

Reaction of B$_5$H$_8$P(H)(CH(OSiMe$_3$)(^{t}Bu)) (3a) with HBF$_4$. In a typical reaction, to 0.2 g (0.6 mmol) of **2a** was added to 20 mL of dried and degassed THF. To this solution was added 1.0 equiv of HBF$_4$. The reaction mixture was stirred at room temperature for 4 h and the solvent removed in vacuo. ^{11}B NMR analysis of the residue showed only unreacted **2a**.

Attempted Elimination Reaction of B$_5$H$_8$P(SiMe$_3$)(CH(OSiMe$_3$)(^{t}Bu)) (2a) with Heat, Base, or Fluoride. Several reactions were attempted to eliminate (Me$_3$Si)$_2$O from compound **2a**.

In one set of experiments, several small pieces of sodium hydroxide were added to 0.20 g (0.60 mmol) of **2a** in diglyme. The reaction was stirred at room temperature overnight. Solvent was removed in vacuo, and the residue was found by NMR analysis to be unreacted **2a**.

In another series of experiments, several small pieces of either sodium or potassium hydroxide were added to 0.20 g (0.60 mmol) of **2a** in a reaction flask connected to a vacuum line. The reactor was heated to 150–170 °C and any volatile products were trapped in a cold trap at −196 °C. After 5 h, no volatile compounds were found to be present in the trap and an NMR analysis of the reactor showed only the presence of unreacted compound **2a**. When the trap was then heated to temperatures above 300 °C, compound **2a** decomposed rapidly.

Compound **2a** was also simply heated in the absence of base in an attempt to promote the elimination reaction. At 100 °C for 3 h, no reaction was observed, as analyzed by NMR spectroscopy.

Finally, **2a** was reacted with 1.0 equiv of Bu$_4$NF in THF at room temperature. Again, no reaction was observed, as analyzed by NMR spectroscopy.

Reaction of B$_5$H$_8$P(SiMe$_3$)(CH(OSiMe$_3$)(^{t}Bu)) (2a) with 2,6-Lutidine. In a vacuum-line trap, 0.2 g (0.6 mmol) of **2a** was reacted with an excess (10 mL) of dried and degassed 2,6-lutidine. The reaction was allowed to stand for 12 h at room temperature. ^{11}B NMR analysis showed only unreacted **2a** after this time. The reaction mixture was then heated at 100 °C for 4 h. The reaction was cooled to room temperature and found to contain only cage decomposition products and the H$_3$B·lutidine adduct.

Results

The reaction of silyl-substituted phosphaalkenes 1 with pentaborane(9) under mild reaction conditions results in their high-yield conversion to bridged phosphaborane systems 2. The high yield of this reaction is notable, since other phosphaborane systems have generally been reported in lower yields. Spectroscopic data for the new compounds reported here are presented in Tables I and II. Data for previously reported selected phosphapentaborane systems are presented in Table III for comparative purposes. A complete table of previously reported small phosphaboranes is available as supplemental material. The preparation of 2 by this synthetic pathway represents the first reported reaction of a neutral borane cluster and a low-valent phosphorus system.[17] By contrast, the reaction of compound 1 with the pentaborane anion under a variety of reaction conditions yielded only cage decomposition products. The chemistry and proposed structure of compound 2 is very different from the proposed phosphorus cage-inserted (Me$_3$Si)$_2$C═PB$_5$H$_8$ compound isolated from the reaction of (Me$_3$Si)$_2$C═PCl with the pentaborane(9) anion previously reported.[5]

Compounds **2a** and **2b** have been characterized by multinuclear NMR, FT-IR, mass spectroscopic, and elemental analyses. NMR data for all the compounds discussed here are presented in Table I. The 80-MHz ^{11}B NMR spectra of both **2a** and **2b** are very simlar to one another and consist of three resonances corresponding to

---

(14) Fessler, M. E.; Whelan, T.; Spencer, J. T.; Grimes, R. N. *J. Am. Chem. Soc.* **1987**, *109*, 7416.

(15) Gaines, D. F.; Iorns, T. V. *J. Am. Chem. Soc.* **1967**, *89*, 3375.

(16) Todd, L. J.; Siedle, A. R. *Prog. NMR Spectrosc.* **1979**, *13*, 87.

(17) The reaction chemistry of phosphaalkynes with neutral borane systems: Miller, R. W.; Spencer, J. T. Submitted for publication.

Table II. Infrared Data for Bridging Phosphaborane Systems

compd	IR data, cm^{-1} [a]
P(SiMe$_3$)$_3$	2955 (s), 2897 (s), 2893 (sh), 2801 (sh), 1458 (m), 1402 (m), 1296 (m), 1248 (m), 1215 (sh), 1170 (w), 1064 (m), 985 (m), 841 (s), 744 (m), 625 (s)
1a, (Z isomer)	2961 (s), 2903 (s), 2872 (sh), 1479 (m), 1460 (m), 1394 (m), 1358 (m), 1296 (s), 1246 (s), 1192 (s), 1053 (s), 904 (s), 827 (s), 758 (s), 690 (m), 625 (m)
1b (Z isomer)	1275 (s), 1253 (vs), 1241 (m), 1215 (vs), 1098 (w), 878 (s), 845 (vs), 835 (vs), 758 (m), 751 (m), 625 (w), 445 (w)
2a	2956 (s, ν_{CH}), 2899 (m, ν_{CH}), 2868 (m, ν_{CH}), 2580 (s, ν_{BH}), 2533 (sh, ν_{BH}), 2519 (s, ν_{BH}), 2365 (w, ν_{BH}), 1472 (m), 1460 (m), 1377 (s), 1359 (s), 1249 (s), 1151 (w), 1080 (s), 1020 (m), 970 (m), 899 (m), 863 (sh), 836 (s), 783 (w), 750 (s), 625 (m), 592 (w), 473 (s)
2b	2953 (sh, ν_{CH}), 2902 (s, ν_{CH}), 2848 (s, ν_{CH}), 2577 (s, ν_{BH}), 2531 (sh, ν_{BH}), 2513 (s, ν_{BH}), 2426 (sh, ν_{BH}), 2381 (sh, ν_{BH}), 1710 (m), 1604 (w), 1495 (w), 1451 (s), 1404 (m), 1358 (s), 1344 (s), 1328 (s), 1313 (s), 1261 (sh), 1251 (s), 1186 (w), 1155 (w), 1131 (w), 1099 (sh) 1077 (s), 976 (m), 940 (w), 918 (w), 870 (sh), 840 (s, br), 755 (m), 729 (m), 693 (m), 625 (w)
3a	2956 (s, ν_{CH}), 2900 (br, ν_{CH}), 2867 (m, ν_{CH}), 2587 (m, ν_{BH}), 2541 (m, ν_{BH}), 2400 (w, ν_{PH}), 1474 (w), 1459 (w), 1410 (w), 1361 (m), 1255 (s), 1152 (sh), 1090 (s), 1023 (m), 969 (w), 931 (w), 899 (w), 861 (sh), 841 (s) 802 (m), 758 (m), 727 (w), 688 (w), 659 (w), 583 (w), 529 (w)
3b	2956 (sh, ν_{CH}), 2930 (sh, ν_{CH}), 2905 (s, ν_{CH}), 2850 (m, ν_{CH}), 2588 (m, ν_{BH}), 2534 (m, ν_{BH}), 2342 (sh, w, ν_{BH}), 2255 (m, ν_{BH}), 2381 (w, ν_{PH}), 1635 (w), 1448 (s), 1311 (w), 1254 (m), 1223 (sh), 1196 (m), 1103 (sh), 1075 (m), 1029 (sh), 878 (sh), 844 (s), 801 (s), 754 (sh), 655 (m), 547 (w)
4a	2955 (s, ν_{CH}), 2899 (w, ν_{CH}), 2863 (m, ν_{CH}), 2582 (m, ν_{BH}), 2537 (s, ν_{BH}), 1741 (w, ν_{PD}), 1472 (w), 1460 (w), 1410 (sh), 1390 (m), 1360 (m), 1333 (w), 1296 (m), 1245 (s), 1160 (w), 1079 (s), 1024 (w), 964 (w), 906 (m), 858 (sh), 837 (s), 804 (w), 754 (m), 683 (m), 650 (sh), 595 (w)
4b	2952 (sh, ν_{CH}), 2923 (sh, ν_{CH}), 2898 (s, ν_{CH}), 2845 (m, ν_{CH}), 2581 (m, ν_{BH}), 2536 (s, ν_{BH}), 2249 (w, ν_{BH}), 1720 (w, ν_{PD}), 1442 (s), 1406 (m), 1355 (w), 1336 (w), 1306 (w), 1243 (s), 1200 (w), 1180 (w), 1124 (m), 1088 (w), 1061 (w), 975 (w), 908 (m), 859 (m), 836 (s), 793 (w), 770 (w), 743 (m), 680 (w), 647 (w), 538 (w), 495 (w)
5a	2957 (s, ν_{CH}), 2923 (s, ν_{CH}), 2851 (m, ν_{CH}), 2584 (m, ν_{BH}), 2535 (m, ν_{BH}), 2442 (w, ν_{BH}), 2394 (w, ν_{BH}), 1457 (m), 1386 (w), 1366 (m), 1330 (w), 1254 (s), 1154 (sh), 1088 (s), 1029 (m), 964 (w), 929 (w), 900 (sh), 863 (m), 843 (s), 800 (m), 757 (m), 696 (w), 654 (w), 618 (w)
7a[b]	2960 (s, ν_{CH}), 2931 (m, ν_{CH}), 2901 (m, ν_{CH}), 2867 (m, ν_{CH}), 2591 (s, ν_{BH}), 2539 (s, ν_{BH}), 2404 (w, ν_{PH}), 1940 (m, ν_{HBH}), 1870 (m, ν_{HBH}), 1509 (sh), 1477 (w), 1463 (w), 1413 (sh), 1376 (s), 1360 (w), 1324 (w), 1255 (s), 1214 (w), 1185 (w), 1100 (sh), 1048 (sh), 969 (w)

[a] NaCl plates. Abbreviations: vs = very strong; s = strong; m = medium; w = weak; sh = shoulder; br = broad. [b] In CDCl$_3$.

the two sets of basal borons and one unique apical boron in 2:2:1 relative intensities. The B–H$_t$ (t = terminal) coupling for the two sets of basal boron resonances were not resolved and consisted of relatively broad, featureless peaks (the average width at half-height for these resonances was 275 Hz in the decoupled spectra). Since other bridged phosphaboranes reported both in this paper and previously[3] show this coupling, the lack of resolution in these basal boron resonances was unusual. One possible explanation of this broadness could be attributed to the presence of endo–exo isomers in the sample that were not independently resolved. Variable-temperature NMR experiments (between 100 and −100 °C), prolonged heating (at 100 °C), and long-term standing under nitrogen (over 1 month) at room temperature did not result in a change in the spectrum. If the presence of endo–exo isomers[18] that are not separated by large barriers to interconversion were the cause of this apparent broadening, then it would have been expected that these experiments would either have resolved the resonances or converted one of the isomers predominantly into the other over time, on the basis of established precedents in the literature.[2-4] An alternative explanation for this broadness could be that the compound exhibited similar values for B–H$_t$ and B–P$_{br}$ (br = bridging) coupling, which, when superimposed in the spectrum, results in the observed broadness.[3] This explanation is also not favored, however, because no significant changes in the spectrum were observed in decoupling experiments. A third possible explanation arises from the fact that all the basal boron atoms of the cage are formally inequivalent due to the presence of a chiral center at the carbon atom attached to the phosphorus. Thus, although B(4) and B(5) are chemically inequivalent, they are in very similar chemical environments and would be expected to display very similar chemical shifts. This also applies to the B(2) and B(3) set of resonances. The broadness of the peaks in the observed spectrum then arises from the failure to resolve these very similar peaks within the B(4)–B(5) and B(2)–B(3) sets. The best apparent rationalizations for the broadness of the basal boron spectral resonances are either that unresolved endo–exo isomers are indeed present in the sample which are not readily interconverted due to the extreme steric bulk and electronic character of the groups attached to the phosphorus atom or else that all four basal borons are inequivalent due to the positioning of the chiral C(R)(H)(OSiMe$_3$) group relative to the cage with hindered rotation around the P–C linkage. The first of these explanations require the restricted rotation of the substituents at the phosphorus atom. From Figure 1, it is clear that, due to the extreme steric bulk of these substituents, restricted rotation at the phosphorus is a very reasonable expectation. The downfield apical boron resonance was, however, resolved into a doublet with J_{BH} coupling of 152 Hz. ^{1}H NMR data for **2** are similar to that expected for a bridged phosphaborane system.[3] The resonances for the three bridging protons were observed as a broad peak centered at about −1.75 ppm. The chemical shifts and coupling observed for the exopolyhedral groups attached to the phosphorus were as expected. ^{13}C NMR data also provide support for our structural assignment of **2**.

The electron-impact mass spectrum of **2** exhibited the expected parent envelope region whose relative intensities corresponded well with those calculated from the isotopic abundances of the elements in the structure.[19] The parent envelope was readily observed in the 11-eV EI spectrum but was not observed at higher ionization energies. Two additional fragments were also prominent in the spectrum and were assigned to the parent fragment minus the C(OSiMe$_3$)(R)H group and the C(OSiMe$_3$)(R)H group itself. Fragment intensity envelopes for each of these other two fragments were also consistent with calculated intensities.

The minimum energy isomer calculated for **2a** was the endo isomer by approximately 26.6 kJ mol^{-1} and is shown

---

(18) The endo isomer is defined as that isomer having the C(R)(H)(OSiMe$_3$) group directed under the open face of the cage.

(19) Ditter, J. F.; Gerhart, F. J.; Williams, R. E. *Mass Spectroscopy of Inorganic Compounds*; ACS Monograph Series 7L; American Chemical Society: Washington, DC, 1968; p 191.

Table III. Compound Data for Selected Previously Reported Phosphapentaborane Systems

compd	^{11}B data,[a] ppm	^{1}H data,[b] ppm	other NMR data, ppm	yield	ref
$((CH_3)PCl)B_5H_8$ (P bridged)	isomer A,[d] −1.0 (d, B(4,5)), −24.2 (t, B(2,3), J_{BH} = 88 Hz), −45.4 (d, B(1)) isomer B,[d] 0.2 (d, B(4,5)), −8.7 (t, B(2,3), J_{BH} = 88 Hz), −46.0 (d, B(1))			ca. 90% but unstable	4, 5
$((Ph)PCl)B_5H_8$ (P bridged)	isomer A,[d] −0.1 (d, B(4,5)), −21.7 (t, B(2,3), J_{BH} = 93 Hz), −43.7 (d, B(1)) isomer B,[d] −0.1 (d, B(4,5)), −9.9 (t, B(2,3), J_{BH} = 93 Hz), −45.5 (d, B(1))				5
$((CHPh_2)$-$PCl)B_5H_8$ (P bridged)	isomer A,[d] −0.5 (d, B(4,5)), −21.8 (t, B(2,3), J_{BH} = 88 Hz), −44.8 (d, B(1)) isomer B,[d] −0.5 (d, B(4,5)), −10.0 (t, B(2,3), J_{BH} = 88 Hz), −45.8 (d, B(1))				5
$((CH(SiMe_3)_2)$-$PCl)B_5H_8$ (P bridged)	isomer A,[d] −0.1 (d, B(4,5)), −17.4 (t, B(2,3), J_{BH} = 88 Hz), −44.5 (d, B(1)) isomer B,[d] −0.1 (d, B(4,5)), −8.8 (t, B(2,3), J_{BH} = 93 Hz), −46.4 (d, B(1))			42%	5
$H_2CPB_5H_8$ (P Inserted)	26.6[d] (d, B(4,5), J_{BH} = 164 Hz), 8.3[d] (d, B(3,6), J_{BH} = 141 Hz), −36.9[d] (d, B(1), J_{BH} = 152 Hz)				5
$(Ph_2)CPB_5H_8$ (P Inserted)	26.6[d] (d, B(4,5), J_{BH} = 161 Hz), 8.9[d] (d, B(3,6), J_{BH} = 146 Hz), −35.3[d] (d, B(1), J_{BH} = 161 Hz)				5
$(Me_3Si)_2CPB_5H_8$ (P Inserted)	23.3[d] (d, B(4,5), J_{BH} = 156 Hz), 6.9[d] (d, B(3,6), J_{BH} = 142 Hz), −39.9[d] (d, B(1), J_{BH} = 141 Hz)		$\delta(^{31}P) = +209$		5
1-(CF_3SPCF_3)-B_5H_8 (P terminal)	27.2[a] (s, B(2)), 27[a] (d, B(3,5), J_{BH} = 155), 33[a] (d, B(4), J_{BH} = 170), 70.2[a] (d, B(1), J_{BH} = 180)				4
$Me_2PB_5H_8$ (P bridged)	19.1[a] (d, B(4,5), J_{BH} = 156 Hz), 41.3[a] (d, B(2,3), J_{BH} = 114 Hz), 64.8[a] (d, B(1), J_{BH} = 154 Hz)	−1.72 (CH_3, J_{PH} = 12 Hz), −1.09 (CH_3, J_{PH} = 10 Hz)	$\delta(^{31}P) = 85$,[c] $\delta(^{19}F) = 59$, J_{PF} = 68 Hz	90% of LiB_5H_8	3
$Me(CF_3)PB_5H_8$ (P bridged)	isomer A, 19.8[a] (d, B(4,5), J_{BH} = 160 Hz), 41.2[a] (d, B(2,3), J_{BH} = 105 Hz), 63.7[a] (d, B(1), J_{BH} = 163 Hz)	isomer A, −1.37 (CH_3, J_{PH} = 10 Hz)	isomer A, $\delta(^{31}P) = 33.5$,[c] $\delta(^{19}F) = 59$, J_{PF} = 68 Hz	91% of LiB_5H_8	3
	isomer B, 18.6[a] (d, B(4,5), J_{BH} = 164 Hz), 41.1[a] (d, B(2,3), J_{BH} = 112 Hz), 64.2[a] (d, B(1), J_{BH} = 163 Hz)	isomer B, −1.97 (CH_3, J_{PH} = 12.6 Hz)	isomer B, $\delta(^{31}P) = 47$,[c] $\delta(^{19}F) = 71$, J_{PF} = 61 Hz		

[a] Positive values are reported upfield from $B(OMe)_3$. [b] Positive values are reported downfield relative to TMS. [c] Positive values are reported upfield relative to 85% H_3PO_4. [d] Relative to BF_3–OEt_2 = 0 ppm.

in Figure 1a.[1] In addition, the bridged structure was lower in energy than the corresponding inserted structure by approximately 112.5 kJ mol^{-1}. In both the bridged and inserted structures, all the bond lengths and angles calculated were consistent with comparable parameters in crystallographically determined analogues. We have presented in the accompanying paper a complete MO (MNDO) treatment of small phosphaborane systems.[1]

Attempts to induce the elimination of $Me_3SiOSiMe_3$, $HSiMe_3$, or other silyl species from **2** by base-induced, fluoride-induced, or thermally induced elimination to prepare the phosphorus cage-inserted compound, either $(R)HC{=}PB_5H_8$ or $(R)(Me_3SiO)C{=}PB_5H_8$, were unsuccessful. This elimination reaction was not observed with conditions similar to those used for the facile elimination of $Me_3SiOSiMe_3$ from phosphaalkenes to form phosphaalkynes.[10]

The reaction of sodium hydride with **2a** resulted in the deprotonation of the cage at a bridging position to prepare the corresponding anion, **5a**. This anion was relatively stable at room temperature, decomposing only slowly to a variety of larger borane cages. Compound **2b**, however, did not react with sodium hydride to form the corresponding anion, presumably because of the extreme stereochemical crowding of the adamantyl group under the cage, which effectively blocked the reaction. This explanation is supported by the previously observed inverse relationship between the rate of bridging proton deprotonation of small carborane systems and the stereochemical bulk of the exopolyhedral substituents on the cage.[14] The rates of deprotonation were also found to be relatively insensitive to electronic influences of the cage and substitutents. Compound **5a** did not react with metal halides, such as $NiBr_2$ and $FeCl_2$, under forcing conditions to produce metallaphosphaborane complexes. The failure of this reaction is atypical of *nido*-borane anions in general and was apparently caused by the large steric requirement of the $[C(OSiMe_3)(H)(^tBu)]$ group under the open face of the borane cage, which effectively blocked the metal's close approach to the nido face.

Compound **2** was found to exhibit relatively high thermal and air stability but was readily and quantitatively converted into compound **3** by either exposure to moisture or reaction with alcohols. The minimum energy structure calculated by MNDO for the endo isomer[18] of **3a** is shown in Figure 1B. In this conversion of **2** to **3**, electrophilic attack at the phosphorus center results in the elimination of either trimethylsilyl alcohol or trimethylsilyl methyl ether and the protonation of the phosphorus center. This electrophilic reaction chemistry has been observed in the reaction of other silylphosphine systems with water in which secondary phosphines are produced, as shown in eq 1.[20] Becker has also shown that phosphaalkenes undergo

$$Me_3SiPEt_2 \xrightarrow{H_2O} Et_2PH + Me_3SiOH \qquad (1)$$

---

[20] Armitage, D. A. In *Comprehensive Organometallic Chemistry*; Wilkinson, G., Stone, F. G. A., Abel, E., Eds; Pergamon: Oxford, England, 1982: Chapter 9.1, p 147.

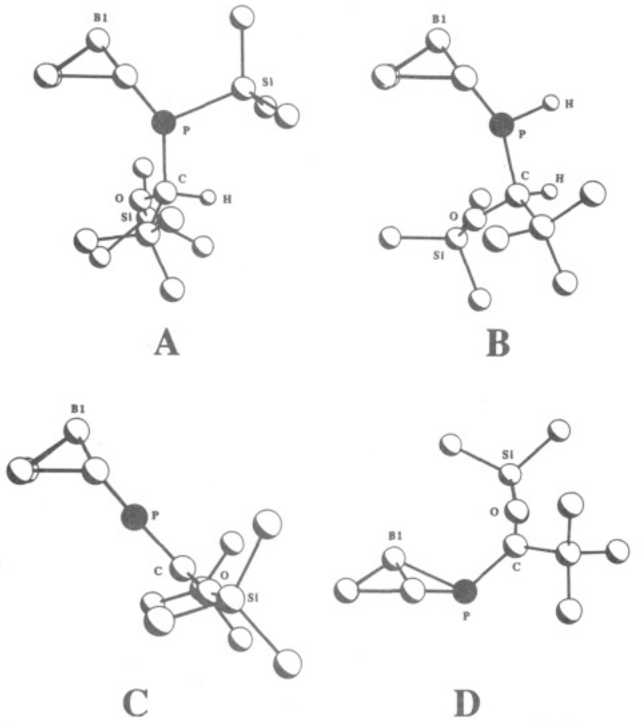

Figure 1. MNDO-calculated minimum energy geometry for several small phosphaboranes. The protons on the borane cage and methyl groups have been omitted for clarity. The views are projections down the B(2)–B(3) axis. Structure A is that of endo-**2a**. The protection of the nido face of the cage by the extreme steric bulk of the C(OSiMe$_3$)(H)(^{t}Bu) group on the phosphorus is apparent in this view. Structure B is that of endo-**3a**. The SiMe$_3$ group on the phosphorus has been replaced by the less sterically demanding proton, which allows the B-(2,3)–P–C angle to increase to relieve some of the steric strain associated with the orientation of the C(OSiMe$_3$)(H)(^{t}Bu) group under the cage. Structure C is that of bridged **6a**. This view shows that the substituents on the carbon are approximately in the B(2)–P–B(3) plane and that the B(2,3)–P–C angle has increased to become approximately linear relative to endo-**3a**. Structure D is that of inserted **6a**. The insertion of the phosphorus into the borane cage results in the deflection of the C(OSiMe$_3$)(H)(^{t}Bu) group above the basal plane, which results in the introduction of significant steric crowding between B(1) and the OSiMe$_3$ group.

a similar reaction with alcohols to produce secondary phosphine centers adjacent to an organic carbonyl group, as shown in reaction 2.[21] The reaction of **2** with D$_2$O

(2)

yields, as expected, the deuterium derivative **4**. The interconversion between **3** and **4** was, however, not observed under any reaction conditions, indicating that once the proton is attached to the phosphorus, it is relatively inert to substitution. The ^{11}B NMR spectra of compounds **3** and **4** are very similar to each other and to that of **2**, with the exception that the P–B coupling of basal B(2) and B(3) atoms to the bridging phosphorus is resolved into a doublet (J_{PB} = ca. 80 Hz) in the proton-decoupled spectra and a pseudotriplet in the coupled spectra. The resonances for the other basal boron atoms in **3** were also resolved into a B–H coupled doublet (J_{PH} = ca. 155 Hz) in the proton-coupled spectra and a singlet in the decoupled spectra. Terminal BH coupling is also observed for the apical boron resonance, as was observed in **2**. The ^{1}H NMR spectrum for **3** clearly shows the absence of the SiMe$_3$ group and the presence of the phosphorus–proton linkage (J_{PH} = 410 Hz). This coupling is also observed in the ^{31}P NMR proton-coupled spectrum. In addition, J_{HPCH} coupling between vicinal protons can be resolved for **3**. In the reaction of **2** with D$_2$O, the ^{1}H spectrum of the product, **4**, again shows the disappearance of the SiMe$_3$ resonance but does not show any vicinal coupling in the CH resonance, as expected from the proposed structure. The infrared spectrum of **3** clearly shows a P–H vibrational mode at 2400 cm^{-1}, which shifts, as expected, to 1741 cm^{-1} upon substitution of the proton with deuterium in compound **4**.

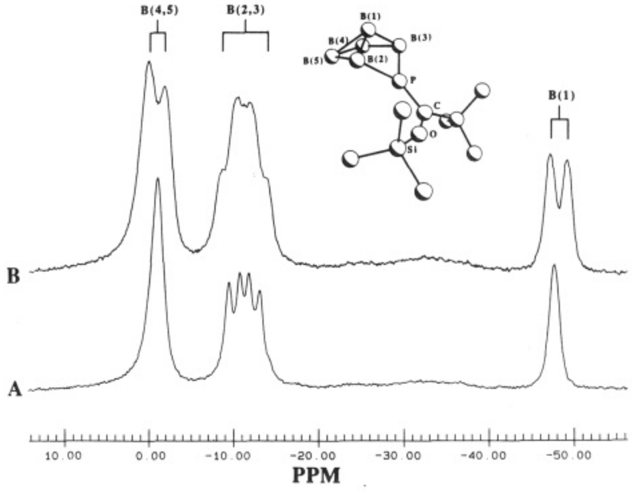

Figure 2. 80-MHz ^{11}B NMR spectra for bridged B$_5$H$_8$P=C-(^{t}Bu)(OSiMe$_3$) (**6a**) in CDCl$_3$ relative to BBr$_3$ (40.0 ppm): (A) ^{11}B{^{1}H} spectrum showing the inequivalence of the two basal borons attached to the phosphorus atom; (B) coupled spectrum showing superposition of the B–P and B–H$_t$ coupling in the two basal borons attached to the phosphorus. Basal boron atoms B(4,5) and the unique apical atom B(1) show simple B–H$_t$ doublets.

The direct involvement of the lone pair of electrons on the phosphorus atom in the bonding of the cage by two 2-center-2-electron B–P interactions, as previously postulated by Burg[3,4] and Gaines,[5] was supported by our inability to access any lone-pair reactivity at the phosphorus center. This was demonstrated by various phosphorus protonation attempts using anhydrous noncoordinating acids, such as HBF$_4$.

Compound **3a**, on standing at room temperature, slowly eliminated hydrogen gas to form compound **6a**, which is proposed as a P=C bridged phosphaborane system. This reaction is shown in eq 3. The structure proposed for **6a** as that of a bridged phosphaborane compound rather than an inserted system[5] is based on several lines of reasoning. The calculated MNDO minimum energy geometries for the bridged and inserted structures for **6a** are shown in Figure 1(c,d, respectively). In eq 3 and Figure 1, it can be seen that the plane of the R–C–R′ system (where R = OSiMe$_3$ and R′ = ^{t}Bu) is approximately coplanar with the B(2)–P–B(3) plane. In this system, boron atoms B(2) and B(3) are, therefore, expected to be inequivalent, since B(3) is closest to the ^{t}Bu group and B(2) is closest to the OSiMe$_3$

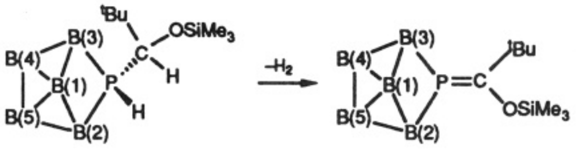

3a **6a**

(3)

---

[21] Becker, B.; Rossler, M.; Uhl, W. *Z. Anorg. Allg. Chem.* **1981**, *473*, 7.

group on the exopolyhedral carbon atom. The inequivalence of B(2) and B(3) requires hindered rotation about the P=C bond, as would be expected for a multiply bonded P=C bond. This inequivalence is readily observed experimentally in the ^{11}B NMR spectrum, as shown in Figure 2. The two sets of resonances for B(2) and B(3) in **6a** are significantly shifted downfield from the B(2,3) resonances in **3a** ($\Delta\delta$ = 9.7 and 12.1 ppm), and each is coupled both to a terminal proton (J_{BH} = 152 and 147 Hz) and to the bridging phosphorus atom (J_{BP} = 111 and 97 Hz). The observation of B–P coupling supports a bridged structure rather than the inserted structure, since B–P coupling in small phosphaboranes is usually observed only in bridged systems and not in cage-inserted cases.[5,6] In addition, the B–P coupling observed for **6a** is significantly larger than that found for **3a**. This indicates that the phosphorus atom uses considerably more 3s atomic orbital character in the bridging B–P–B bonding interaction in compound **6a**. This results directly from the necessity for the phosphorus to use a higher atomic 3p contribution in the bonding to the exopolyhedral carbon atom, as would be expected in the formation of a P=C double pπ–pπ bond on going from **3a** to **6a**. The ^{1}H NMR spectrum of **6a** is quite similar to that of **3a** with the conspicuous absence of the P–H and C–H resonances. The absence of the proton on the phosphorus is also apparent from the ^{31}P NMR spectrum. In the ^{13}C{^{1}H} NMR spectrum of **6**, the R and R′ resonances are also quite similar to those in compound **3a**. The PC resonance is, however, shifted approximately 68.9 ppm further downfield from that observed for **3a**. This shift represents an approximate split of the difference between the singly bonded P–C μ-phosphaborane system, **3a**, and the resonance for the free phosphaalkene, **1a**. This clearly indicates the formation of multiple-bond character in the P–C linkage of **6a**. Gaines has reported a N=C bridged system from the reaction of nitriles with pentaborane.[22] The ^{11}B NMR spectrum for this compound is similar to that observed for **6a** ($B_5H_8N{=}CH(^tBu)$, ^{11}B NMR δ 1.4 (d, J_{BH} = 156 Hz), −2.3 (d), −4.6 (d), −51.5 (d, J_{BH} = 161 Hz)) and significantly different from the spectrum of the proposed inserted P=C system (Table III). Finally, MNDO calculations of both the bridged and inserted structures show that the bridged system lies approximately 32.5 kJ mol^{-1} lower in energy than the inserted structure.

Compound **3a** can be readily deprotonated by sodium hydride to prepare the corresponding anion **7a**. The rate of the deprotonation for **3a** was significantly greater than that observed for **2a**. This observation is again consistent with the reported relationship between steric bulk and rate of deprotonation, since the stereochemical crowding in **3a** is significantly reduced relative to **2a** by the replacement of a $SiMe_3$ group with a proton on phosphorus.[14] Compound **7a** reacted readily with metal halides to give metallaphosphaborane complexes, which will be reported in a subsequent paper.[23]

Discussion

The facile preparation of the synthetically versatile small phosphaborane compounds **2** and **3** provides an important pathway into cage and exopolyhedral reaction chemistry (Scheme I). It also allows for the systematic study of some of the factors controlling the relationship between bridged and cage-inserted structures.

The failure of compound **1a** to eliminate $Me_3SiOSiMe_3$ upon reaction with the neutral pentaborane(9) cluster under a variety of reaction conditions was unexpected in light of both the reported conversion of $(Me_3Si)_2C{=}PCl$ to the cluster-inserted product, $[(Me_3Si)_2C{=}PB_5H_8]$,[5] and the well-known base-promoted elimination of $Me_3SiOSiMe_3$ by silyl-substituted phosphaalkenes in the preparation of phosphaalkynes.[24] In fact, no elimination reactions were observed for any of these new systems, with the exception of the loss of hydrogen from **3** to give **6**. With respect to this latter reaction, MNDO calculations for compound **3a** show the proton on the phosphorus atom to be partially positively charged and the proton on the adjacent carbon to be partially negatively charged. This arrangement is apparently well set up for the elimination of hydrogen to produce the novel unsaturated bridging phosphaborane **6**.

Two generally similar mechanistic pathways can be postulated to account for the reactivity patterns demonstrated by phosphaalkenes with neutral borane clusters. These proposed mechanistic pathways are shown in Scheme II. In the first pathway, the lone pair of electrons on the phosphorus center is proposed to initially attack at a basal boron position of the neutral pentaborane(9) cage system. This results in the formation of a phosphorus–boron bond and a hydride shift from an adjacent bridging position to a terminal position on a neighboring basal boron to form a BH_2 unit. This shift can then be followed by the transfer of a terminal proton from this BH_2 unit to the relatively electronegative carbon center of the phosphaalkene unit, essentially resulting in the hydroboration of the phosphaalkene bond. As a result of this rearrangement, a highly basic boron center is generated at the previous BH_2 site adjacent to the phosphorus–boron linkage (indicated by a pair of unshared electrons in the scheme). The close proximity of the relatively electropositive phosphorus center to this basic site allows the "ring-closure" reaction to readily occur by the attack of this electron-rich boron atom on the phosphorus atom to form the boron–phosphorus–boron bridged system. This final closure provides the observed $[\mu\text{-}(P(SiMe_3)C(OSiMe_3)(H)(R))B_5H_8]$ product. Data from MNDO calculations provide clear support for this mechanism. These calculations show that in the free phosphaalkene, the phosphorus center is electron-rich relative to its adjacent carbon atom (calculated charges: phosphorus, −1.120; carbon, +0.445).[25] The Lewis base coordination would be expected to occur exclusively at a basal site of the neutral pentaborane(9) molecule, since these boron atoms are significantly more electropositive than the apical boron atom (MNDO charges calculated in our work for B_5H_9 of B_{bas} = +0.028 and B_{ap} = −0.318 (bas = basal; ap = apical) corresponded in sign with those previously reported).[26] This is also consistent with the synthetic work reported by Burg[27] and Kodama[6d] in the preparation of terminal phosphine-substituted pentaboranes. Upon formation of the P→B donor bond, the phosphorus atom of the coordinated phosphaalkene becomes more positive relative to the free molecule, directing the proton-transfer reaction to the relatively electron-rich carbon center. This proton transfer is supported by Lipscomb's determination that basal boron atoms of B_5H_9 bonded to two terminal protons were significantly more positive than those bonded to only

---

[22] Coons, D. E. Ph.D. Dissertation, The University of Wisconsin—Madison, Madison, WI, 1984.

[23] Miller, R. W.; Cendrowski, S.; Spencer, J. T. Work in progress.

[24] Regitz, M.; Binger, P. *Angew. Chem., Int. Ed. Engl.* **1988**, *27*, 1484.

[25] Glass, J. A., Jr.; Spencer, J. T. Work in progress.

[26] Switkes, E.; Epstein, I. R.; Tossell, J. A.; Stevens, R. M.; Lipscomb, W. N. *J. Am. Chem. Soc.* **1970**, *92*, 3837.

[27] Burg, A. B. *CHEMTECH* **1977**, *50*.

Scheme I. Synthesis and Reactivity of Small Bridging Phosphaborane Systems[a]

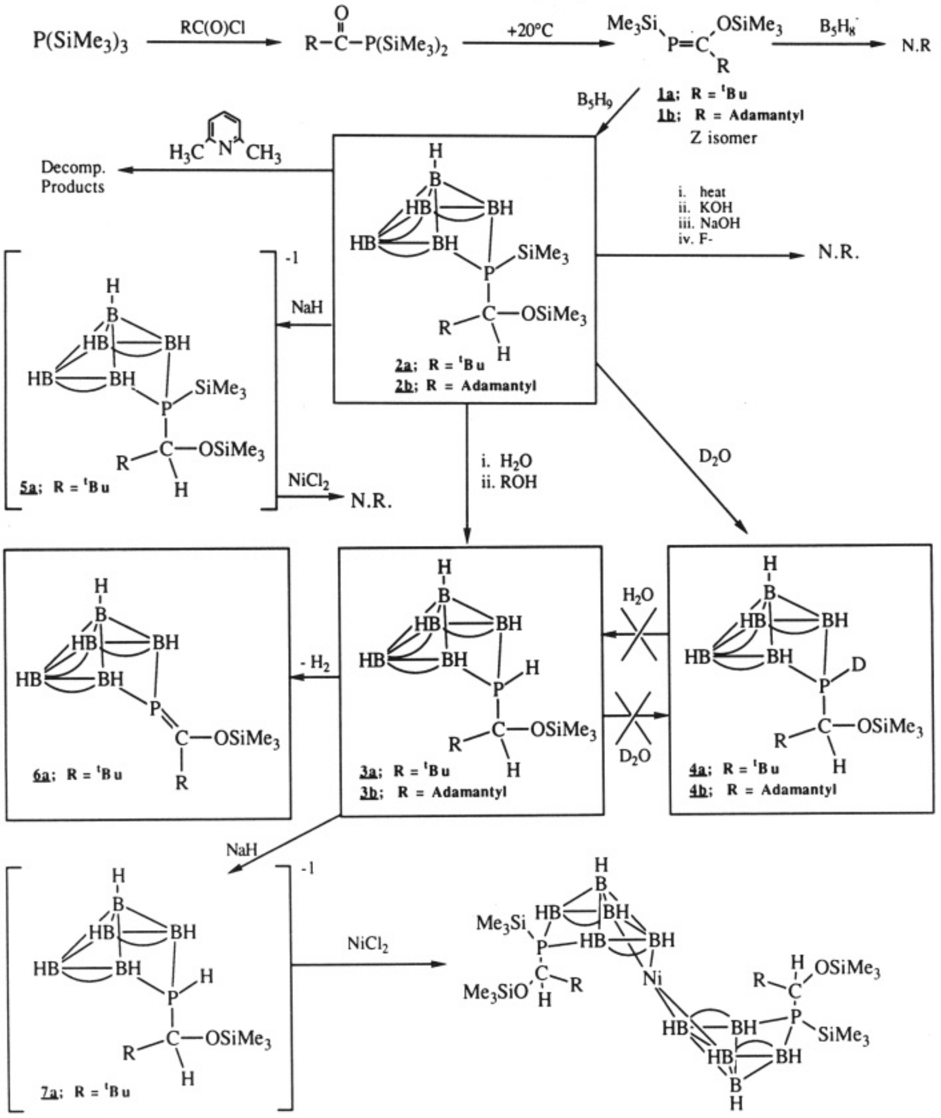

[a] Bridging cage protons indicated by small arcs attaching appropriate boron atoms.

Scheme II. Proposed Mechanisms for the Reaction of Neutral Boranes and Phosphaalkenes in the Formation of Bridged Phosphaborane Systems

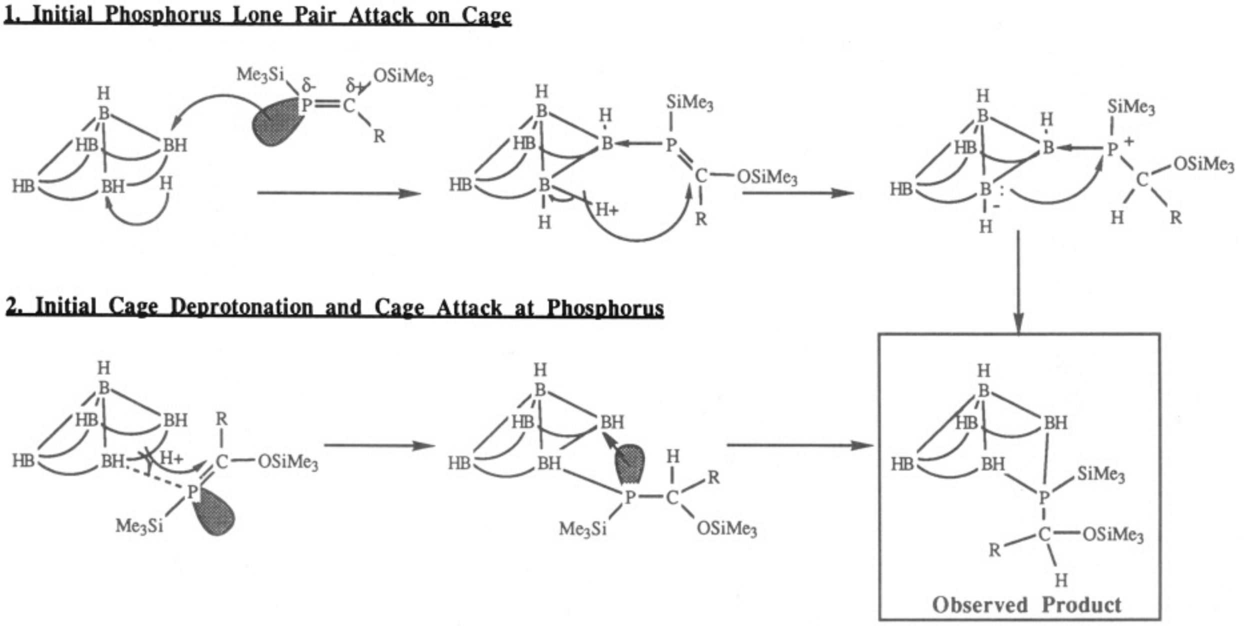

one proton.[26] This charge distribution provides a driving force for the transfer of the proton from the $BH_{2(t)}$ to the electronegative carbon atom. It has also been shown that electron-withdrawing substituents on carborane cages promote the acidity of the cage protons.[14] By similar reasoning, the final closure step is then expected to be directed to the phosphorus center. In the first step of this mechanism, it is apparent that the phosphaalkene molecule is not sufficiently basic to remove a BH_3 unit from the cage in a simple acid–base adduct reaction. This BH_3 removal reaction has been observed in our work, however, to readily occur in the reaction between $P(SiMe_3)_3$ and pentaborane(9). In the second proposed mechanistic pathway, the initial step is presumed to involve a proton shift from the cage to the carbon center of the incoming phosphaalkene concurrent with the formation of a phosphorus–boron bond. This step is indeed similar to the penultimate step of the first mechanism in which the cage acts as a strong nucleophile and attacks the electropositive phosphorus center of the phosphaalkene. In the final step of this second mechanism, the lone pair of electrons on the phosphorus attacks at an adjacent borane cage site to accomplish the ring closure and to produce the observed product. This mechanistic pathway can be related to that proposed by Sneddon et al.[28] for the incorporation of a CN unit into a borane cluster from the reaction of *arachno*-$S_2B_7H_8^-$ anion with nitriles. In that mechanism, the first step is proposed to involve the nucleophilic attack of the thiaborane anion on the relatively electropositive carbon atom of the polarized nitrile, followed by the hydroboration of the nitrile bond. As a consequence of this interaction, the lone pair of electrons on the pendant imino group becomes strongly nucleophilic and attacks at the most electropositive center of the thiaborane cage. This lone-pair interaction forces a cage rearrangement and closes the cage ring system to produce the observed "bridging" nitrile system. While this mechanism is clearly favored for anionic borane systems with highly polarized reactants, problems occur with its application to the neutral cage systems. In the case of our second neutral borane–phosphaalkene mechanism presented above, MNDO calculations appear to be less supportive for this pathway than for the first mechanism. The initial step would require the transfer of a proton from the cage to the relatively electropositive carbon atom of the phosphaalkene reactant while requiring the nucleophilic attack of a basal boron atom at the relatively electron-rich phosphorus center. In the second step, attack of the relatively weakly donating lone pair of electrons on phosphorus, since it now has a partially positive character, at an adjacent basal boron to accomplish the final ring-closure reaction is required. From this argument, the first mechanism must clearly be favored over the second in the case of neutral borane systems.

It seems reasonable to suggest that phosphaborane preparation reactions, such as those described above, may indeed involve either or both of these mechanisms, with the proportion of the reaction occurring by any particular pathway governed by the choice of starting reagents. The reaction of strongly nucleophilic borane systems, such as borane anions, with polarizable systems would be expected to occur predominantly by the second mechanism proposed. Additionally, this mechanism would be presumed to be the most important in the reactions involving either systems that do not possess lone-pair electrons or those in which the lone pair is only weakly basic. In contrast, the reaction of neutral boranes with good nucleophiles should proceed predominantly by the first reaction pathway.

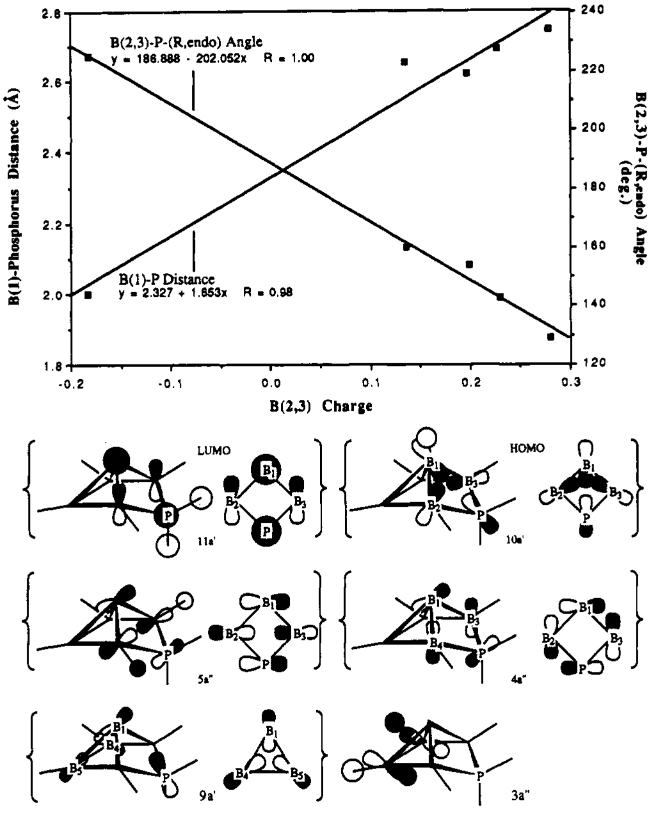

Figure 3. Correlation between the calculated charge at bridgehead boron atoms and the MNDO-calculated B(1)–P distance and the B(2,3)–P–(R_{endo}) bond angle. Plotted are the data for compounds endo-**2a**, exo-**2a**, endo-**3a**, endo-**5a**, and inserted **6a**. (Those compounds with hydrogen atoms in the endo positions are omitted.)

It should be possible to alter the final structure of the product to provide end-bridged (such as compound **2**), side-bridged (such as [*hypho*-5-CH_3-5,11,7,14-$CNS_2B_7H_9$][28] and [μ-($(CH_3)_2NCH_2$)B_5H_8]),[29] or inserted systems depending upon the relative polarities and nucleophilicities of the systems to be reacted with the borane cages. Investigations into the reactions of these types of systems, such as RP=PR, RP=BR ("reversed polarity"), and phosphaalkynes, are currently in progress.

MNDO calculations have provided a great deal of insight into the predicted structures and properties of these small phosphaborane systems. We have previously presented a complete MO bonding description for end-bridged and inserted small phosphaborane systems.[1] In the MNDO calculations for the compounds reported here, an additional structural trend was observed, as shown in Figure 3. Linear trends were observed between the calculated charge on the bridgehead basal boron atoms and both the phosphorus–apical boron bond distance and the bridgehead basal boron bond centroid–phosphorus–carbon bond angle. This indicates that as the charge on the bridgehead boron atoms becomes more negative and the phosphorus becomes more positive, the structure tends toward an inserted structure with the phosphaalkene carbon atom

---

(28) Sang, O. K.; Furst, G. T.; Sneddon, L. G. *Inorg. Chem.* **1989**, *28*, 2339.

(29) Coons, D. E.; Gaines, D. F. *Inorg. Chem.* **1986**, *25*, 364.

(30) Barron, A. R.; Cowley, A. H.; Hall, S. W. *J. Chem. Soc., Chem. Commun.* **1987**, 980.

(31) Fritz, v. G.; Holderich, W. *Z. Anorg. Allg. Chem.* **1976**, *422*, 104.

(32) Burg, A. B.; Mishra, I. B., *J. Organomet. Chem.* **1970**, *24*, C33.

(33) Maya, L.; Burg, A. B. *Inorg. Chem.* **1974**, *13*, 1522.

deflected toward the apical boron above the basal plane. These trends can possibly be understood by considering the fact that as the charge on phosphorus increases, the 10a′ (HOMO) molecular orbital, which is phosphorus–apical boron antibonding in character, is destabilized (shown in Figure 3). The 5a″ orbital, which is phosphorus–apical boron bonding in nature, becomes stabilized and is therefore more important in determining the structure adapted. The calculated variation of the energies of the molecular orbitals in these small phosphaborane systems with changes in the (basal boron plane)–(bridgehead boron–phosphorus plane) dihedral angle clearly shows these trends.[1]

Acknowledgment. We wish to thank the National Science Foundation (Grant No. MSS-89-09793), the donors of the Petroleum Research Fund, administered by the American Chemical Society, the General Electric Co., the Rome Air Development Center (Award No. F30602-89-C-0113), IBM, and the Industrial Affiliates Program of the Center of Molecular Electronics for support of this work. We also wish to thank Mr. John A. Glass, Jr., for assistance with MNDO calculations included in this work.

Supplementary Material Available: A table of complete MNDO-calculated bond lengths, bond angles, interplane dihedral angles, energy terms, and internal charge distribution data for compounds **2a** (endo and exo), **3a** (endo and exo), **5a** (endo and exo), and **6a** (bridged and inserted) and a complete listing of compound data for previously reported small phosphaborane systems (^{11}B, ^{1}H, ^{13}C, ^{31}P, and ^{19}F NMR, mass spectroscopic, and yield data) (6 pages). Ordering information is given on any current masthead page.

Cp*MoO$_2$Cl-Catalyzed Epoxidation of Olefins by Alkyl Hydroperoxides

Mary K. Trost and Robert G. Bergman*

Department of Chemistry, University of California, Berkeley, California 94720

Received August 6, 1990

Irradiation of Cp*Mo(CO)$_3$Cl in the presence of oxygen affords the Mo^{VI} oxo complex Cp*MoO$_2$Cl (**5**). Complex **5** was found to act as a catalyst of the reaction of alkyl hydroperoxides and olefins to yield the corresponding epoxides and alcohols. No oxidation of the pentamethylcyclopentadienyl ligand of **5** was observed under the conditions of the epoxidation reaction. The characteristics of the epoxidation reaction catalyzed by **5** is similar to that of other Mo^{VI} catalysts. In the absence of added olefins, **5** reacts with alkyl hydroperoxides to yield the peroxo complex Cp*Mo(O$_2$)OCl (**6**). The peroxo complex **6** is inert to reaction with olefins, thus ruling out **6** as the intermediate responsible for olefin oxidation in this system. An investigation of the relative rate of epoxidation of cyclohexene, 1-methylcyclohexene, and 1,2-dimethylcyclohexene with various alkyl hydroperoxides demonstrates that the relative rates depend on the structure of the alkyl group of the alkyl hydroperoxide. This result demonstrates that the alkyl hydroperoxide is incorporated in the transition state for the oxygen-transfer step of the reaction.

Introduction

Molybdenum complexes are well-established catalysts for the epoxidation of olefins by alkyl hydroperoxides.[1] The usefulness and practicality of this reaction has been demonstrated by the success of the Halcon process, which is the molybdenum-catalyzed oxidation of propylene to propylene oxide by *tert*-butyl hydroperoxide.[2] Because of both the economic and scientific value of this reaction, it has been studied intensively.

Many molybdenum species are known that catalyze the epoxidation reaction, and in all cases, the active species is believed to be a Mo^{VI} compound.[1b] The coordination environment generally contains hard electronegative ligands such as oxide, carboxylate, chloride, and amide ligands, which are stable to the oxidizing conditions of the epoxidation reaction. Some problems exist in identifying the active catalyst in the epoxidation reactions. Often the original molybdenum complex is converted to its active form under the reaction conditions. This is best illustrated by Mo(CO)$_6$, which is a convenient source of molybdenum

Chart I

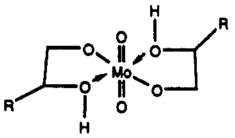

1

R = CH$_3$, n-C$_6$H$_{13}$

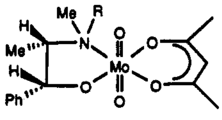

2

R = CH$_3$, CH$_2$CH$_3$

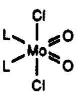

3a L = Dimethylformamide (DMF)
3b L = Hexamethylphosphorous triamide (HMPT)

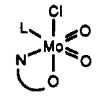

4

L = Hexamethylphosphorous triamide
N---O = pyridine-2-carboxylate
or 8-hydroxyquinolinate

Scheme I

---

[1] For reviews concerning transition-metal catalysis of the epoxidation reaction, see: (a) Mimoun, H. *J. Mol. Catal.* **1980**, *7*, 1. (b) Sheldon, R. A. *J. Mol. Catal.* **1980**, *7*, 107. (c) Sharpless, K. B.; Verhoeven, T. R. *Aldrichim. Acta* **1979**, *12*, 63. (d) Sheldon, R. A.; Kochi, J. K. *Metal Catalyzed Oxidations of Organic Compounds*; Academic: New York, 1981. (e) Lyons, J. E. *Aspects Homogeneous Catal.* **1977**, *3*, 1. (f) Sobczak, J.; Ziolkowski, J. J. *J. Mol. Catal.* **1981**, *13*, 11.

[2] Landau, R.; Sullivan, G. A.; Brown, D. *CHEMTECH* **1979**, 602.

0276-7333/91/2310-1172$02.50/0